International Journal of Heat and Mass Transfer 52 (2009) 2079–2091

Contents lists available at ScienceDirect

International Journal of Heat and Mass Transfer

journal homepage: www.elsevier.com/locate/ijhmt

A three-dimensional inverse geometry problem in estimating the space and time-dependent shape of an irregular internal cavity

Cheng-Hung Huang *, Chi-An Chen

Department of Systems and Naval Mechatronic Engineering, National Cheng Kung University, Tainan 701, Taiwan, ROC

ARTICLE INFO

Article history:
Received 13 July 2008
Received in revised form 23 October 2008
Available online 16 December 2008

ABSTRACT

A three-dimensional inverse geometry problem (or shape identification problem) to estimate the unknown space and time-dependent irregular shape of internal cavity by utilizing the gradient-based steepest descent method (SDM) and a general purpose commercial code CFD-ACE+ is considered in the present study. The validity of the present inverse algorithm is examined based on the simulated measured temperature distributions on the outer surface by an imaginary infrared scanner. The advantage of calling CFD-ACE+ as a subroutine in this shape identification problem lies in its characteristics of automatic mesh generation since this function of CFD-ACE+ enables the easily-handling of the moving boundary problem. Two numerical test cases are performed to test the validity and accuracy of the present shape identification algorithm by using different types of cavity shapes, initial guesses and measurement errors. Results show that excellent estimations on the unknown geometry of the internal cavity can be obtained.

1. Introduction

The inverse geometry problems or shape identification problems have become another area of active research recently and many researchers have used infrared scanners in their applications to perform the nondestructive evaluation (NDE) (Hsieh and Su [1]). The inverse geometry problems require a complete regeneration of the mesh as the geometry evolves. Moreover, the continuous evolution of the geometry itself poses certain difficulties in arriving at analytical or numerical solutions. For this reason it is necessary to use an efficient solver such that the above mentioned nature of this problem can be handled, especially for the three-dimensional applications.

The inverse geometry problems, including the cavity or shape estimation, are based on either steady or unsteady-state response of a body subjected to boundary heat fluxes or thermal sources. The steady-state problems have been solved by a variety of numerical methods (Hsieh and Kassab [2], Kassab and Hsieh [3], Hsieh, Choi and Liu [4], Kassab and Pollard [5], Dems and Mroz [6,7], Burczinski, Kane, and Balakrishna [8], Burczynski, Beluch, Dlugosz, Kus, Nowakowski, and Orantek [9], Cheng and Wu [10]).

Huang and his co-workers have utilized the conjugate gradient method (CGM) and steepest descent method (SDM) to the inverse geometry problems and have published a series of relevant papers. The SDM and CGM are also called the iterative regularization method, which means the regularization procedure is performed during the iterative processes and thus the determination of optimal regularization conditions is not needed. The SDM and CGM derive from the perturbation principles and transforms the shape identification problem to the solution of three problems, namely, the direct, sensitivity and adjoint problems.

Huang and Chao [11] first derived the formulations with CGM in determining the unknown irregular boundary configurations for a two-dimensional, steady-state shape identification problem. Huang and Tsai [12] adopted the previous algorithm in Huang and Chao [11] and extended it to a transient shape identification problem in identifying the unknown irregular boundary configurations from external measurements. Huang, Chiang and Chen [13] have developed a new algorithm for a two-dimensional multiple cavities estimations where the search directions are not confined in one direction, i.e. the unknown parameters become x- and I-coordinates. Huang and Hsiung [14] applied the same algorithm in determining the optimal shape of cooling passages for gas turbine. Huang and Chen [15] extended the similar algorithm to a multiple region domain in estimating the time and space varying outer boundary configurations. Huang and Chaing [16] applied the technique of SDM to a shape identification problem in estimating the boundary configurations in a three-dimensional domain. In Huang and Chaing [16], the direction of descent is restricted to only one direction and therefore its algorithm cannot be applied to estimate the shape of cavity, unless some modifications are made.

It should be noted that the above references, except for Huang and Chaing [16], are all the two-dimensional shape identification problems; the three-dimensional shape identification problems

* Corresponding author.
E-mail address: chhuang@mail.ncku.edu.tw (C.-H. Huang).

0017-9310/$ - see front matter © 2008 Elsevier Ltd. All rights reserved.
doi:10.1016/j.ijheatmasstransfer.2008.10.024

Nomenclature

C_p	heat capacity
$f(x,y,z,t)$	unknown irregular cavity configuration
J	functional defined by Eq. (2)
J'	gradient of functional defined by Eq. (13)
k	thermal conductivity
q_o	heat flux density
S_i	inner surface of cavity
S_o	outer boundary surface
t	time
$T(x,y,z,t)$	estimated temperature
$\Delta T(x,y,z,t)$	sensitivity function defined by Eq. (5)
$Y(x,y,z,t)$	measured temperature

Greeks

β	search step size defined by Eq. (7)
Ω	computational domain
$\lambda(x,y,z,t)$	Lagrange multiplier defined by Eq. (10)
$\delta(\bullet)$	Dirac delta function
ω	random number
ε	convergence criterion
ρ	density
σ	standard deviation of the measurement errors

Superscript

^	estimated values
n	iteration index

are still very limited in the literatures. Recently, Divo, Kassab and Rodriguez [17] have used a singular superposition technique and the genetic algorithm for detecting the unknown cavity in a three-dimensional steady inverse geometry problem. In their study the shape of a three-dimensional cavity is only a sphere, not an arbitrary shape and not a function of time, and the convergent speed for the genetic algorithm is also slow.

The objective of this work is to extend the algorithm of previous studies by the authors, Huang and Chao [11], Huang and Tsai [12] and Huang and Chaing [16] to estimate the unknown three-dimensional, space and time-dependent shape for internal cavity by utilizing SDM and CFD-ACE+ code [18] as the subroutine to solve this three-dimensional shape identification problem. The unknown parameters become the x, y and z-coordinates of the cavity with time and this implies that there is huge number of unknowns in the present study.

The commercial code CFD-ACE+ is a power tool in the field of advanced computational fluid dynamics and has the feature of auto mesh, it can be used to calculate many practical but difficult direct thermal problems. If one can devise one algorithm which has the ability to communicate with CFD-ACE+ by means of data communication, a generalized three-dimensional shape identification problem can thus be established.

The above mentioned direct, sensitivity and adjoint problems can be solved by CFD-ACE+ and the calculated values are used in SDM for shape identifications. The bridge between CFD-ACE+ and SDM is the INPUT/OUTPUT files. Those files should be arranged such that their format can be recognized by CFD-ACE+ and SDM. A sequence of forward transient heat conduction problems is solved by CFD-ACE+ in an effort to update the cavity geometry by minimizing a residual measuring the difference between estimated and measured temperatures at the temperature extracting locations on the outer surface under the present algorithm.

The numerical experiments for this study with two different irregular cavity geometries will be illustrated to show the validity of using SDM in the present transient three-dimensional shape identification problem.

2. The direct problem

The following three-dimensional, time-dependent inverse geometry problem is considered here to show the methodology for use in determining the unknown internal cavity geometry in a homogeneous medium.

For a domain Ω, initially the temperature is kept as a constant $T = T_\infty$, the boundary condition on inner cavity surface S_i is subjected to the prescribed temperature condition $T = T_i$. The boundary condition on outer boundary surface S_o is subjected to a known heat flux q_o. Fig. 1 shows the geometry and the coordinates for the transient three-dimensional physical problem considered here. The mathematical formulation of this time-dependent heat conduction problem with the shape of internal cavity unknown is given by:

$$k\left[\frac{\partial^2 T}{\partial^2 x}+\frac{\partial^2 T}{\partial^2 y}+\frac{\partial^2 T}{\partial^2 z}\right]=\rho C_p\frac{\partial T}{\partial t};\quad \text{in}\quad \Omega,\quad t>0 \tag{1a}$$

$$T=T_i;\quad \text{on inner cavity surface } S_i=f(x,y,z,t),\quad t>0 \tag{1b}$$

$$\pm k\frac{\partial T}{\partial \xi}=q_o;\quad \text{on outer boundary surface } S_o,\quad t>0 \tag{1c}$$

$$T=T_\infty;\quad \text{in}\quad \Omega,\quad t>0 \tag{1d}$$

here k, ρ and Cp are the thermal conductivity, density and heat capacity, respectively, and $\frac{\partial T}{\partial \xi}$ represents the temperature gradient along the normal direction of S_o.

The direct problem posted here is concerned with the determination of the medium temperature when the cavity geometry $f(x,y,z,t)$, the initial condition as well as the boundary conditions on all boundary surfaces are known. The commercial package CFD-ACE+ is used to solve the above direct problem.

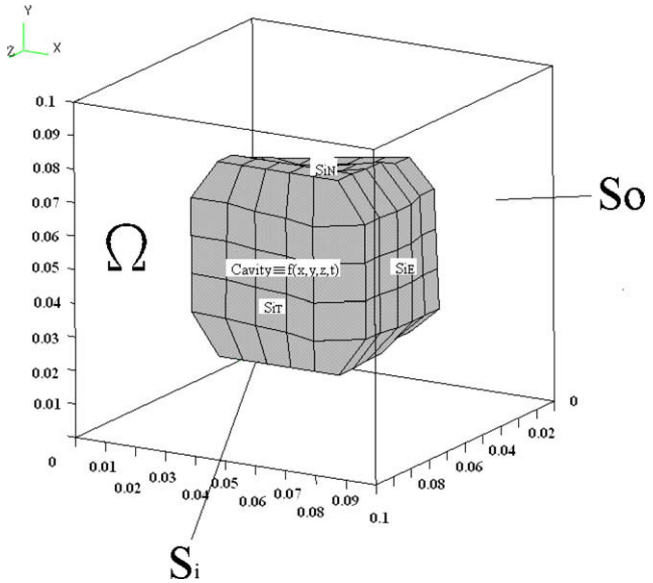

Fig. 1. Geometry and coordinates for the present inverse geometry problem.

3. The inverse geometry problem

For the inverse geometry problem considered here, the space and time-dependent cavity geometry $f(x,y,z,t)$ is regarded as being unknown, but everything else in Eq. (1) is known. In addition, simulated temperature readings taken at some appropriate locations on the outer surface S_o by an imaginary infrared scanner are considered available.

Referring to Fig. 1, let the simulated temperature reading at time t on outer surface S_o be denoted by $\mathbf{Y}(S_o,t) \equiv Y(x_m,y_m,z_m,t) \equiv Y_m(S_o,t)$, $m = 1$ to M, where M represents the number of position of measured temperature extracting points. This inverse geometry problem can be stated as follows: by utilizing the above mentioned simulated measured temperature data $Y_m(S_o,t)$, estimate the unknown space and time-dependent geometry of the internal cavity $S_i = f(x,y,z,t)$.

The solution of this shape identification problem is to be obtained in such a way that the following functional is minimized:

$$J[f(x,y,z,t)] = \int_{t=0}^{t_f} \sum_{m=1}^{M} [T_m(S_o,t) - Y_m(S_o,t)]^2 dt \tag{2}$$

here T_m are the estimated or computed temperatures at the measurement locations (x_m,y_m,z_m) and time t on S_o. These quantities are determined from the solution of the direct problem given previously by using an estimated cavity for the exact cavity $f(x,y,z,t)$.

4. Steepest descent method for minimization

The steepest descent method (SDM) is similar to but simpler than the conjugate gradient method (CGM) (Alifanov [19]) since the calculations of the conjugate coefficient and direction of descent are not needed. It is found that SDM can achieve our goal in the present inverse geometry problem and converges very fast. The following iterative process based on the SDM is now used for the estimation of the unknown space and time-dependent shape of internal cavity $f(x,y,z,t)$ by minimizing the functional $J[f(x,y,z,t)]$.

$$f^{n+1}(x^{n+1},y^{n+1},z^{n+1},t^{n+1}) = f^n(x^n,y^n,z^n,t^n) - \beta^n J'^n \tag{3a}$$

where

$$J'^n(x,y,z,t) = J'^n_x \vec{i} + J'^n_y \vec{j} + J'^n_z \vec{k} \tag{3b}$$

and $\vec{i},\vec{j}$ and $\vec{k}$ indicate the directional vectors for x, y and z directions, respectively, or more explicitly

$$x^{n+1} = x^n - \beta^n J'^n_x(x,y,z,t) \tag{4a}$$
$$y^{n+1} = y^n - \beta^n J'^n_y(x,y,z,t) \tag{4b}$$
$$z^{n+1} = z^n - \beta^n J'^n_z(x,y,z,t) \tag{4c}$$

and

$$f^{n+1}(x,y,z,t) = f(x^{n+1},y^{n+1},z^{n+1},t) \tag{4d}$$

here β^n is the search step size in going from iteration n to iteration n+1, $J'^n(x,y,z,t)$ is the gradient in the outward normal direction while $J'^n_x(x,y,z,t), J'^n_y(x,y,z,t)$ and $J'^n_z(x,y,z,t)$ are the gradients in x, y and z directions, respectively.

To perform the iterations according to Eq. (3), the step size and the gradients of the functional $J'^n_x(x,y,z,t), J'^n_y(x,y,z,t)$ and $J'^n_z(x,y,z,t)$ need be calculated. In order to develop expressions for the determination of these quantities, a "sensitivity problem" and an "adjoint problem" are constructed as described below.

5. Sensitivity problem and search step size

The sensitivity problem for this inverse geometry problem is obtained from the original direct problem defined by Eq. (1) in the following manner: It is assumed that when $f(x,y,z,t)$ undergoes a variation $\Delta f(x,y,z,t)$, $T(x,y,z,t)$ is perturbed by $T + \Delta T$. By replacing in the direct problem f by $f + \Delta f$ and T by $T + \Delta T$, subtracting the resulting expressions from the direct problem and neglecting the second-order terms, the following sensitivity problem for the sensitivity function ΔT can be obtained.

$$k\left[\frac{\partial^2 \Delta T}{\partial^2 x} + \frac{\partial^2 \Delta T}{\partial^2 y} + \frac{\partial^2 \Delta T}{\partial^2 z}\right] = \rho C_p \frac{\partial \Delta T}{\partial t}; \quad \text{in } \Omega,\ t > 0 \tag{5a}$$

$$\Delta T = \Delta f \frac{\partial T}{\partial \xi}; \quad \text{on inner cavity surface } S_i = f(x,y,z,t), \quad t > 0 \tag{5b}$$

$$\frac{\partial \Delta T}{\partial \xi} = 0; \quad \text{on outer boundary surface } S_o, \quad t > 0 \tag{5c}$$

$$\Delta T = 0; \quad \text{in } \Omega, \quad t = 0 \tag{5d}$$

The commercial package CFD-ACE+ can be used to solve the above sensitivity problem. The functional $J(f^{n+1})$ for iteration $n + 1$ is obtained by rewriting Eq. (2) as

$$J[f^{n+1}] = \int_{t=0}^{t_f} \sum_{m=1}^{M} [T_m(f^n - \beta^n J'^n;\ S_o,t) - Y_m]^2 dt \tag{6a}$$

where f^{n+1} has been replaced by the expression given by Eq. (3a). If temperature $T_m(f^n - \beta^n J'^n;\ S_o,t)$ is linearized by a Taylor expansion, Eq. (6a) takes the form

$$J(f^{n+1}) = \int_{t=0}^{t_f} \sum_{m=1}^{M} [T_m(f^n;\ S_o,t) - \beta^n \Delta T_m(J'^n) - Y_m]^2 dt \tag{6b}$$

here $T_m(f^n;S_o,t)$ is the solution of the direct problem at (x_m,y_m,z_m,t) by using estimated shape of cavity for exact f(x,y,z,t). The sensitivity function $\Delta T_m(J'^n)$ is taken as the solution of problem (5) at the measured positions (x_m,y_m,z_m) and time t by letting $\Delta f = J'^n$. The search step size β^n can be determined by minimizing the functional given by Eq. (6b) with respect to β^n. The following expression results:

$$\beta^n = \frac{\int_{t=0}^{t_f} \sum_{m=1}^{M} [(T_m - Y_m)\Delta T_m] dt}{\int_{t=0}^{t_f} \sum_{i=m}^{M} (\Delta T_m)^2 dt} \tag{7}$$

6. Adjoint problem and gradient equation

To obtain the adjoint problem, Eq. (1a) is multiplied by the Lagrange multiplier (or adjoint function) $\lambda(x,y,z,t)$ and the resulting expression is integrated over the correspondent space and time domains. The result is then added to the right hand side of Eq. (2) to yield the following expression for the functional $J[f(x,y,z,t)]$:

$$\begin{aligned} J[f(x,y,z,t)] = {} & \int_{t=0}^{t_f} \sum_{m=1}^{M} (T_m - Y_m)^2 dt \\ & + \int_{t=0}^{t_f} \int_{\Omega} \lambda \left[k\left(\frac{\partial^2 T}{\partial x^2} + \frac{\partial^2 T}{\partial y^2} + \frac{\partial^2 T}{\partial z^2}\right) - \rho C_p \frac{\partial T}{\partial t} \right] \\ d\Omega dt = {} & \int_{t=0}^{t_f} \int_{S_o} [T - Y]^2 \delta(x - x_m)\delta(y - y_m)\delta(z - z_m) dS_o dt \\ & + \int_{t=0}^{t_f} \int_{\Omega} \lambda \left[k\left(\frac{\partial^2 T}{\partial x^2} + \frac{\partial^2 T}{\partial y^2} + \frac{\partial^2 T}{\partial z^2}\right) - \rho C_p \frac{\partial T}{\partial t} \right] d\Omega dt \end{aligned} \tag{8}$$

where $\delta(\bullet)$ is the Dirac delta function. The variation ΔJ is obtained by perturbing f by Δf and T by ΔT in Eq. (1), subtracting the resulting expression from the original Eq. (1) and neglecting the second-order terms. Finally the following expression can be obtained

$$\Delta J[f(x,y,z,t)] = \int_{t=0}^{t_f}\int_{S_o} 2[T-Y]\Delta T\delta(x-x_m)\delta(y-y_m)\delta(z-z_m)\,dS_o dt + \int_{t=0}^{t_f}\int_{\Omega}\lambda\left[k\left(\frac{\partial^2\Delta T}{\partial x^2}+\frac{\partial^2\Delta T}{\partial y^2}+\frac{\partial^2\Delta T}{\partial z^2}\right)-\rho C_p\frac{\partial\Delta T}{\partial t}\right]d\Omega dt \tag{9}$$

here (x_m,y_m,z_m), $m = 1$ to M, refers to the temperature extracting points for imaginary infrared scanners. In Eq. (9), the domain integral term is reformulated based on Green's second identity; the boundary conditions of the sensitivity problem given by Eqs. (5b) and (5c) are utilized and then ΔJ is allowed to go to zero. The vanishing of the integrands containing ΔT leads to the following adjoint problem for the determination of $\lambda(x,y,z,t)$:

$$k\left[\frac{\partial^2\lambda}{\partial^2 x}+\frac{\partial^2\lambda}{\partial^2 y}+\frac{\partial^2\lambda}{\partial^2 z}\right]+\rho C_p\frac{\partial\lambda}{\partial t}=0;\quad \text{in}\quad \Omega,\quad t>0 \tag{10a}$$

$$\lambda = 0;\quad \text{on inner cavity surface } S_i = f(x,y,z,t),\quad t>0 \tag{10b}$$

$$\frac{\partial\lambda}{\partial\xi} = 2(T-Y)\delta(x-x_m)(\delta y-y_m)\delta(z-z_m);\quad \text{on outer boundary surface } S_o,\quad t>0 \tag{10c}$$

$$\lambda = 0;\quad \text{in}\quad \Omega, t=t_f$$

The commercial package CFD-ACE+ is utilized to solve the above adjoint problem. Finally, the following integral term is left

$$\Delta J = \int_{t=0}^{t_f}\int_{S_i} -\left[\frac{\partial\lambda}{\partial\xi}\frac{\partial T}{\partial\xi}\right]\Delta f(x,y,z,t)\,dS_i dt \tag{11a}$$

From definition (Alifanov [19]), the functional increment can be presented as

$$\Delta J = \int_{t=0}^{t_f}\int_{S_i} J'(x,y,z,t)\Delta f(x,y,z,t)\,dS_i dt \tag{11b}$$

A comparison of Eqs. (11a) and (11b) leads to the following expression for the gradient of functional $J'(x,y,z,t)$ of the functional $J[f(x,y,z,t)]$:

$$J'(x,y,z,t) = -\frac{\partial\lambda}{\partial\xi}\frac{\partial T}{\partial\xi}\bigg|_{S_i} = -\left(\frac{\partial\lambda}{\partial x}\frac{\partial T}{\partial x}\bigg|_{S_i}\right)\vec{i}-\left(\frac{\partial\lambda}{\partial y}\frac{\partial T}{\partial y}\bigg|_{S_i}\right)\vec{j}-\left(\frac{\partial\lambda}{\partial z}\frac{\partial T}{\partial z}\bigg|_{S_i}\right)\vec{k} \tag{12}$$

Again, a comparison of Eqs. (3b) and (12) obtain the following gradient equations

$$J'_x(x,y,z,t) = -\frac{\partial\lambda}{\partial x}\frac{\partial T}{\partial x} \tag{13a}$$

$$J'_y(x,y,z,t) = -\frac{\partial\lambda}{\partial y}\frac{\partial T}{\partial y} \tag{13b}$$

$$J'_z(x,y,z,t) = -\frac{\partial\lambda}{\partial z}\frac{\partial T}{\partial z} \tag{13c}$$

The calculation of gradient equation is the most important part of SDM since it plays a significant role of the shape identification calculations.

It is noted that $J'(x,y,z,0)$ and $J'(x,y,z,t_f)$ are always equal to zero since and $\frac{\partial T(x,y,z,0)}{\partial\xi} = 0$. If the initial values of $f(x,y,z,0)$ and final time values of $f(x,y,z,t_f)$ cannot be obtained before the shape identify calculations, the estimated values of $f(x,y,z,t)$ will deviate from the exact values near both initial and final time conditions. This is the case in the present study. However, if we let

$$\frac{\partial T(x,y,z,0)}{\partial\xi} = \frac{\partial T(x,y,z,\Delta t)}{\partial\xi} \tag{14a}$$

$$\frac{\partial\lambda(x,y,z,t_f)}{\partial\xi} = \frac{\partial\lambda(x,y,z,t_f-\Delta t)}{\partial\xi} \tag{14b}$$

where Δt denotes the time increment used in the numerical calculation. By applying Eqs. (14a) and (14b) to the gradient Eq. (13), the singularity at $t = 0$ and t_f can be avoided in the present study, however, the estimations are still not reliable near $t = 0$ and t_f. For this reason the estimations in the beginning and final two time steps will be excluded from the relative error calculations.

7. Stopping criterion

If the problem contains no measurement errors, the traditional check condition specified as follow can be used as the stopping criteria

$$J[f^{n+1}(x,y,z,t)] < \varepsilon \tag{15a}$$

where ε is a small specified number and a monotonic convergence can be obtained with SDM. However, the observed temperature data may contain measurement errors. Therefore, it is not expected that the functional Eq. (2) to be equal to zero at the final iteration step. Following the experience of the author (Alifa-

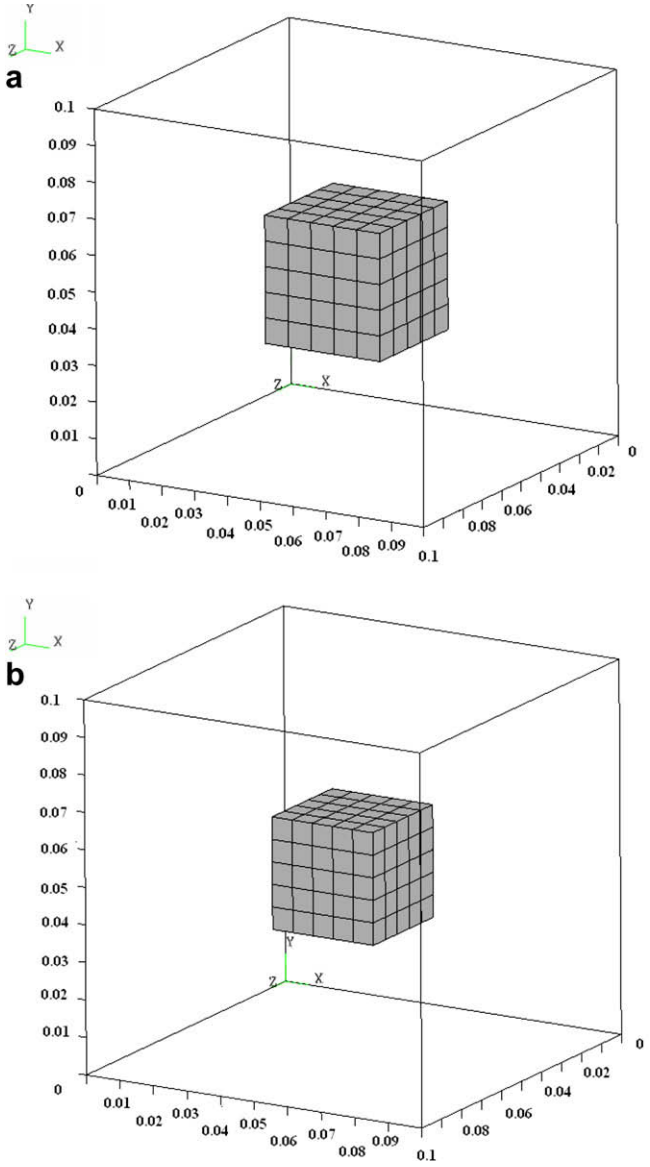

Fig. 2. The (a) type A and (b) type B initial guesses for the shape of internal cavity in the present numerical experiments.

nov [19]), the discrepancy principle is used as the stopping criterion, i.e. it is assumed that the temperature residuals may be approximated by

$$T_m - Y_m \approx \boldsymbol{\sigma} \tag{15b}$$

where σ is the standard deviation of the measurement errors, which is assumed to be a constant. Substituting Eq. (15b) into Eq. (2), the following expression is obtained for ε:

$$\varepsilon = M\sigma^2 t_f \tag{15c}$$

For this reason the stopping criterion is given by Eq. (15a) with ε determined from Eq. (15c).

8. Computational procedure

The computational procedure for the solution of this shape identification problem using SDM can be summarized as follows:

Suppose the estimated $\hat{f}^n(x,y,z,t)$ is available at iteration n

- Step 1. Solve the direct problem given by Eq. (1) for $T(x,y,z,t)$.
- Step 2. Examine the stopping criterion given by Eq. (15a) with ε given by Eq. (15c). Continue if not satisfied.
- Step 3. Solve the adjoint problem given by Eq. (10) for $\lambda(x,y,z,t)$.
- Step 4. Compute the gradients of the functional J'_x, J'_y and J'_z from Eqs. (13a), (13b), and (13c), respectively.
- Step 5. Set $\Delta f(x,y,z,t) = J'^n(x,y,z,t)$, and solve the sensitivity problem given by Eq. (5) for $\Delta T(x,y,z,t)$.
- Step 6. Compute the search step size β^n from Eq. (7).
- Step 7. Compute the new estimation for $\hat{f}^{n+1}(x,y,z,t)$ from Eq. (4) and return to step 1.

9. Results and discussions

To examine and illustrate the validity of this shape identification problem in estimating the space and time-dependent irregular configuration of an internal cavity from the knowledge of the simulated temperature recordings taken by an imaginary

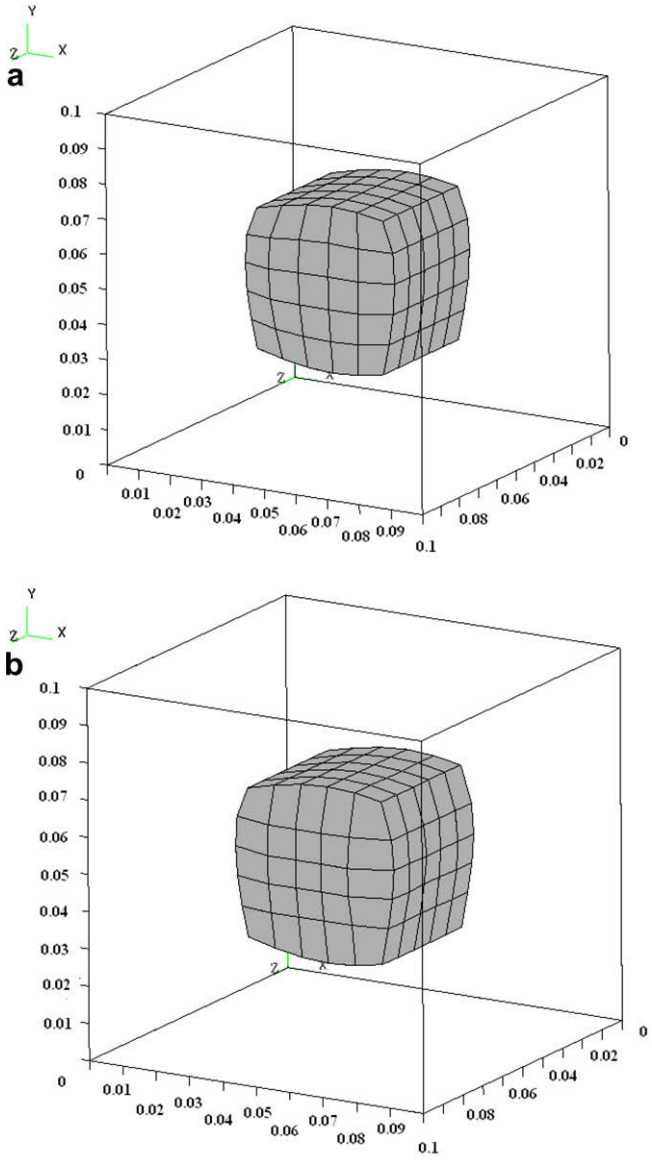

Fig. 3. The (a) exact and (b) estimated cavity configurations with type A initial guess and $\sigma = 0.0$ at time $t = 20$ s in case 1.

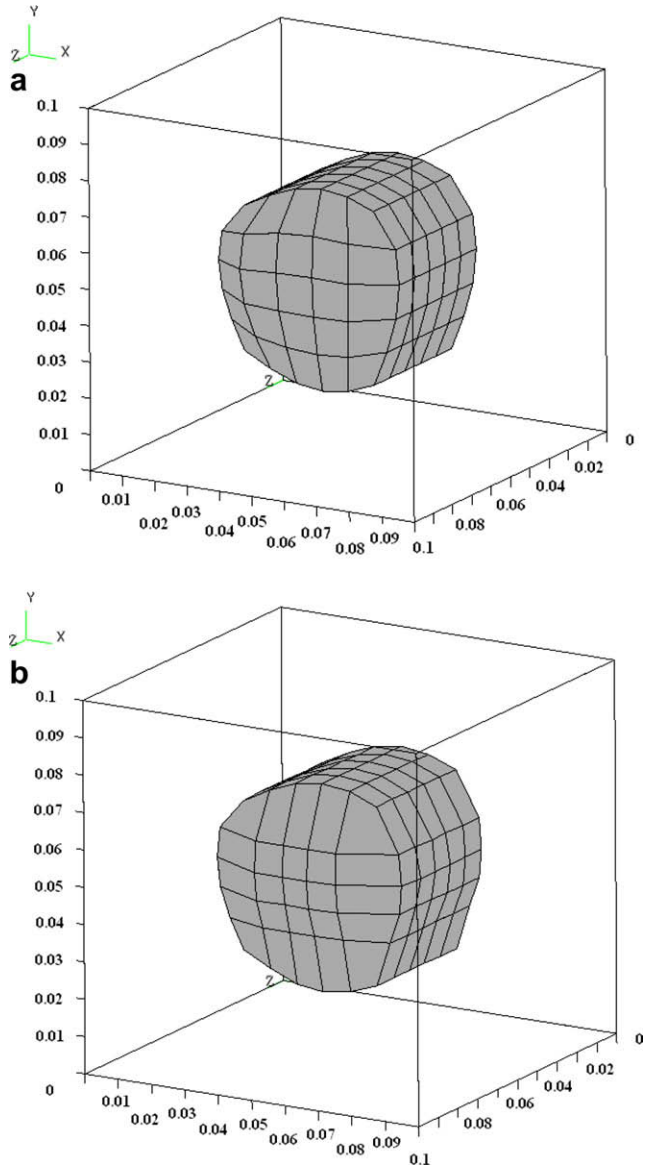

Fig. 4. The (a) exact and (b) estimated cavity configurations with type A initial guess and $\sigma = 0.0$ at time $t = 50$ s in case 1.

infrared scanner on the outer surface S_o, two specific examples are considered where the shape of exact and initial guess cavities are varied.

The dimension of the outer boundary for all the examples considered in this study is taken as a cube with length equal to 10 cm. In all the test cases considered here the following thermal parameters are chosen, $k = 76.2$ W/(m-K), $\rho = 7870$ kg/m^3, Cp = 440 J/(kg-K) and $q = -500$ W/m^2.

In order to construct the grid system for the internal cavity $S_i = f(x,y,z,t)$, it is assumed that S_i is composed by six sub-surfaces, i.e. $S_i = \{S_{iE}, S_{iW}, S_{iS}, S_{iN}, S_{iT}, S_{iB}\}$, where S_{iE}, S_{iW}, S_{iS}, S_{iN}, S_{iT}, S_{iB} represent the east, west, south, north, top and bottom surfaces. The number of grids used for each sub-surface are 6×6, which implies that each sub-surface surface has 36 grid points and therefore there are totally of 152 grid points on both the external surface and inner cavity surface; or $(152 \times 3) = 456$ unknown parameters of x-, y- and z-coordinates in the present case. In time domain, total time is taken as 100 s and $\Delta t = 5$ s is used in numerical calculations. Therefore there is totally of 9576 discreted boundary shapes need to be estimated in this study. The initial temperature T_∞ is chosen as 27 °C and the boundary temperature for inner cavity surface is taken as $T_i = 200$ °C. The measurement surface is always on S_o, i.e. on the outer surfaces.

The goal of this study is to show the accuracy of the present approaches in identifying the inner cavity surface $S_i = f(x,y,z,t)$, with no prior information on the functional form of the unknown cavity, which is the so-called function estimation.

In order to compare the results for situations involving random measurement errors, the normally distributed uncorrelated errors with zero mean and constant standard deviation were assumed. The simulated inexact measurement data $\mathbf{Y}$ can be expressed as

$$\mathbf{Y} = \mathbf{Y}_{dir} + \omega\sigma \tag{16}$$

where $\mathbf{Y}_{dir}$ is the solution of the direct problem with an exact $f(x,y,z,t)$; ω is a random variable that generated by subroutine DRN-

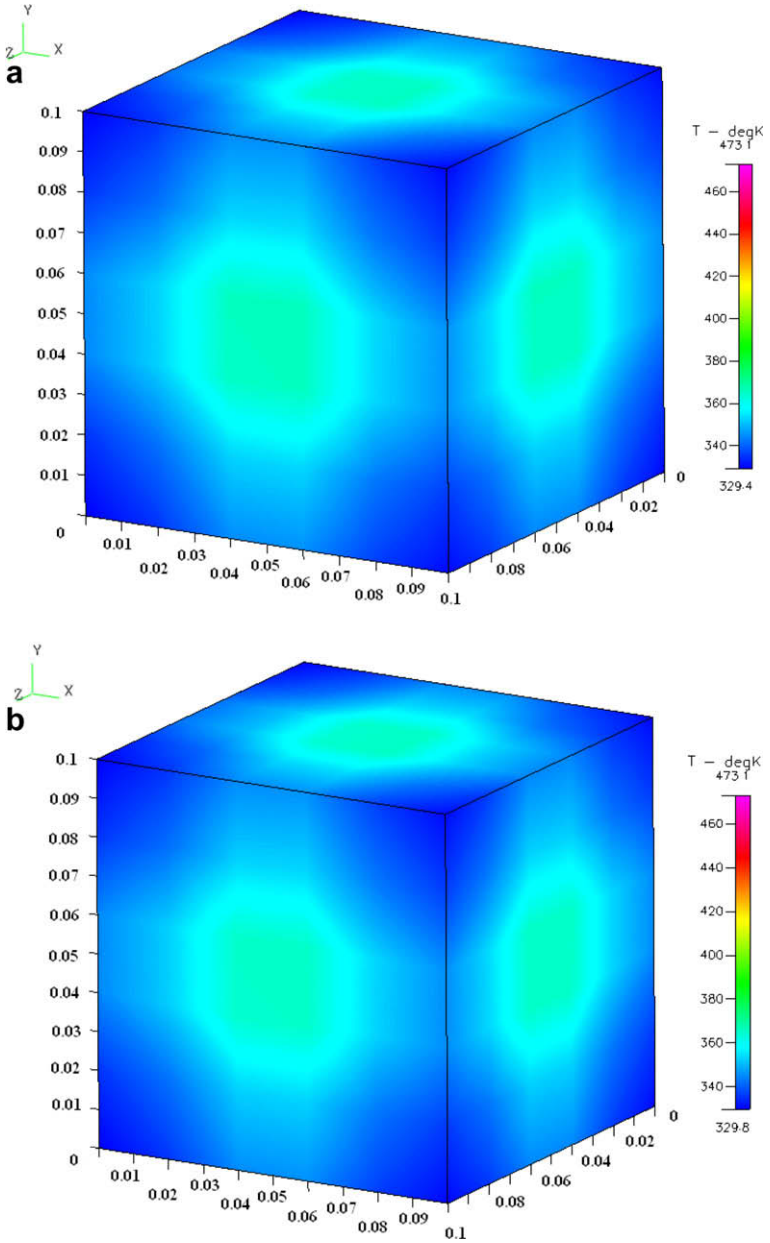

Fig. 5. The (a) simulated measured and (b) estimated surface temperatures on S_o with $\sigma = 0.0$ at time $t = 20$ s in case 1.

NOR of the IMSL [20] and will be within −2.576 to 2.576 for a 99% confidence bounds and σ is the standard deviation of the measurement error.

To examine the effects of different shapes of initial guesses of the cavity to the final estimations, two different shapes of initial guesses are used in this work. The followings define these two types of initial guesses:

Type A: A cube with length equal to 3.5 cm and its center located at (5,5,5) cm.

Type B: A cube with length equal to 3.0 cm and its center located at (5,5,5) cm.

The plots for these two initial guesses of the cavity are shown in Fig. 2a and b, respectively.

One of the advantages of using the SDM is that it does not require a very accurate initial guess of the unknown quantities, this can be verified in the following numerical test cases. Two numerical test cases in identifying the shape of the time-dependent internal cavity $f(x,y,z,t)$ by using the SDM are now presented below.

9.1. Numerical test case 1

The unknown space and time-dependent cavity configuration on $S_i = \{S_{iE}, S_{iW}, S_{iS}, S_{iN}, S_{iT}, S_{iB}\} = f(x,y,z,t)$, is assumed in the following form

$$S_{iE} = 0.07 + \left\{ \frac{\sin[\frac{250}{12}(y-0.03)\pi]}{110} \times \sin\left(\frac{\pi t}{30}\right) \right\} \tag{17a}$$

$$S_{iW} = 0.03 - \left\{ \frac{\sin[\frac{250}{12}(y-0.03)\pi]}{110} \times \sin\left(\frac{\pi t}{30}\right) \right\} \tag{17b}$$

$$S_{iS} = 0.03 - \left\{ \frac{\sin[\frac{250}{12}(x-0.03)\pi]}{110} \times \sin\left(\frac{\pi t}{30}\right) \right\} \tag{17c}$$

$$S_{iN} = 0.07 + \left\{ \frac{\sin[\frac{250}{12}(x-0.03)\pi]}{110} \times \sin\left(\frac{\pi t}{30}\right) \right\} \tag{17d}$$

$$S_{iT} = 0.07 + \left\{ \left[\frac{\sin\frac{250}{12}(y-0.03)\pi}{110} \right] \times \sin\left(\frac{\pi t}{30}\right) \right\} \tag{17e}$$

$$S_{iB} = 0.03 - \left\{ \frac{\sin[\frac{250}{12}(y-0.03)\pi]}{110} \times \sin\left(\frac{\pi t}{30}\right) \right\} \tag{17f}$$

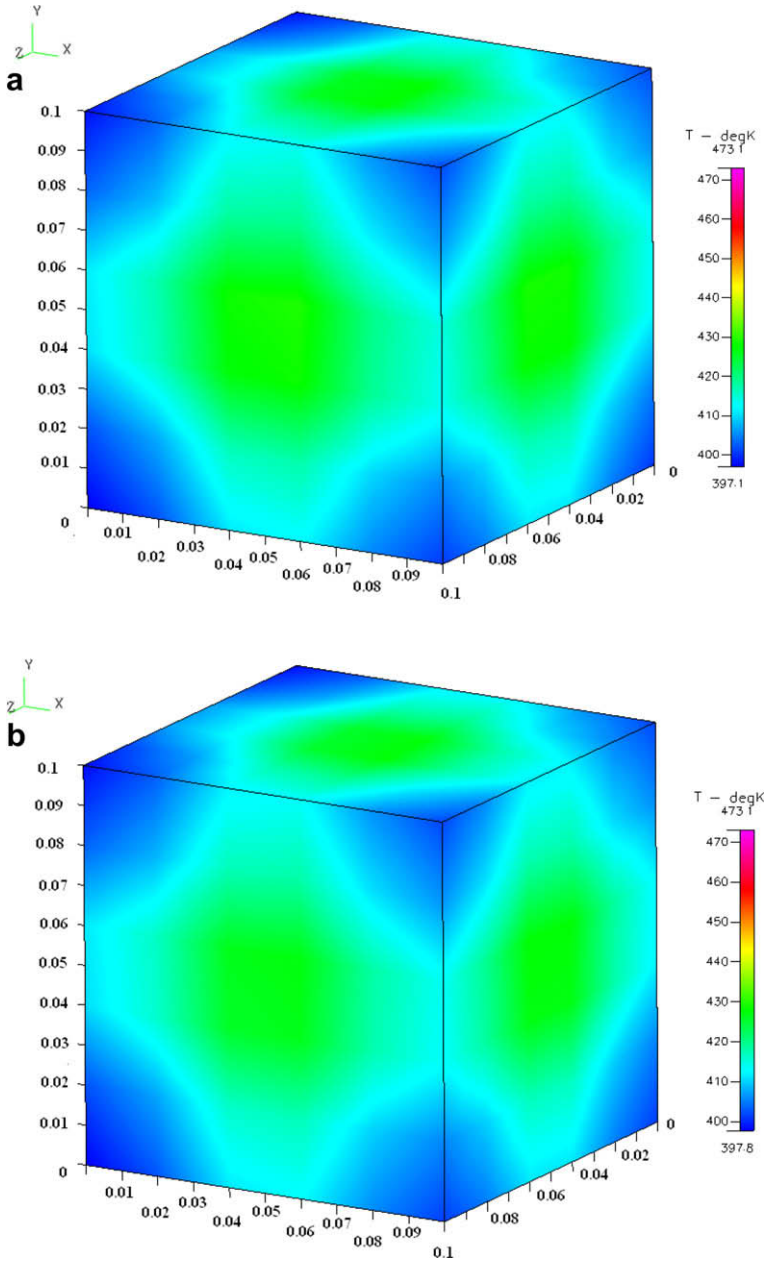

Fig. 6. The (a) simulated measured and (b) estimated surface temperatures on S_o with $\sigma = 0.0$ at time $t = 50$ s in case 1.

First, when assuming exact measurements ($\sigma = 0.0$), using type A initial guess and choosing $\varepsilon = 47500$, after 8 iterations the estimation can be obtained. The CPU time on 586-3.0 GHz PC used in the SDM calculations is about 8 h and 22 min.The average relative errors for the exact and estimated cavity configurations and for the measured and estimated temperatures are calculated ERR1 = 2.66% and ERR2 = 0.42%, respectively, where the average relative errors ERR1 and ERR2 are defined as

$$\mathrm{ERR1} = \sum_{n=2}^{N-2}\sum_{i=1}^{I}\left|\frac{f(x_i,y_i,z_i,t_n)-\hat{f}(x_i,y_i,z_i,t_n)}{f(x_i,y_i,z_i,t_n)}\right| \div \mathrm{I} \div (\mathrm{N}-3)\times 100\% \quad (18a)$$

$$\mathrm{ERR2} = \sum_{n=2}^{N-2}\sum_{m=1}^{M}\left|\frac{T(x_m,y_m,z_m,t_n)-Y(x_m,y_m,z_m,t_n)}{Y(x_m,y_m,z_m,t_n)}\right| \div \mathrm{M} \div (\mathrm{N}-3)\times 100\% \quad (18b)$$

here, $I = 152$, $M = 152$ and $N = 20$ represent the total discreted number of grid on the cavity surface, total number of measurements and the total discreted number of grid on time, respectively, while f and $\hat{f}$ denote the exact and estimated values of cavity configurations, respectively.

The exact and estimated shapes of internal cavity by using SDM at time $t = 20$ s and 50 s are shown in Figs. 3 and 4, respectively and the measured and estimated temperatures for $t = 20$ s and 50 s are presented in Figs. 5 and 6, respectively. ERR1 and ERR2 at $t = 20$ s are calculated as 0.41% and 0.11%, respectively, while at $t = 50$ s are obtained as 1.21% and 0.19%, respectively.

It can be seen from the above figures and relative average errors that the present shape identification scheme obtained good estimation for $f(x,y,z,t)$ since the shape of internal cavity can be reconstructed without assuming any extra conditions.

Next, it would be of interest to examine the accuracy of the estimations when different initial guess is considered. The computational conditions are the same as the previous case except that type B initial guess is now chosen. By choosing $\varepsilon = 47500$ and $\sigma = 0.0$, after 9 iterations the estimated shape of internal cavity

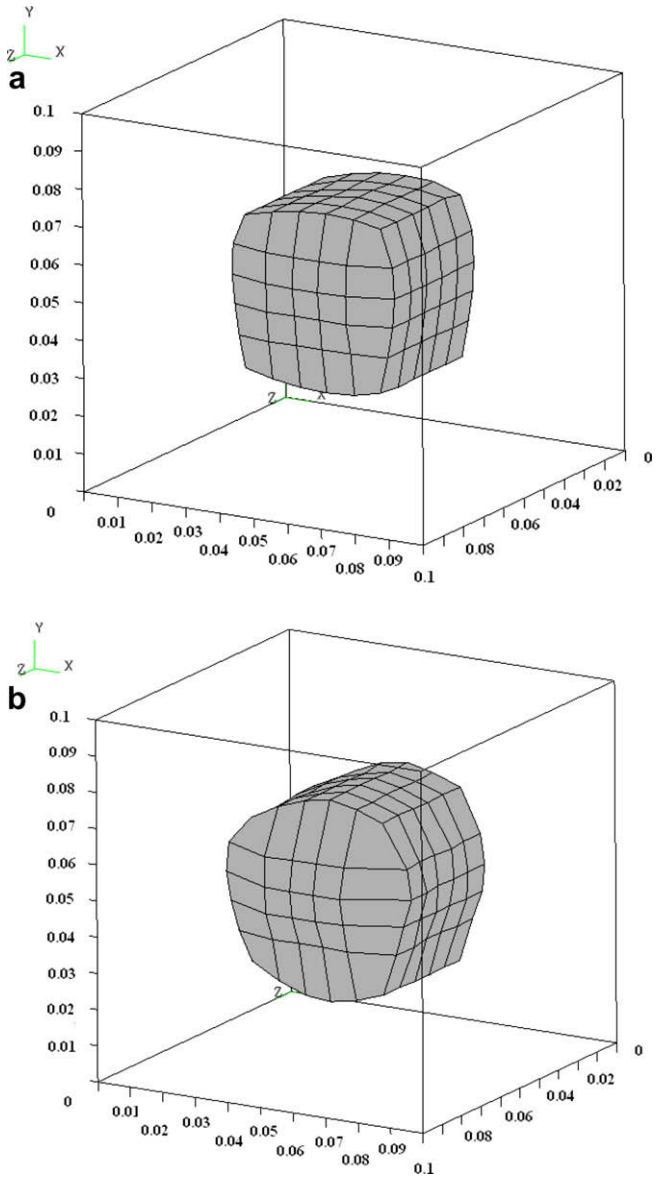

Fig. 7. The estimated cavity configurations with type A initial guess and $\sigma = 3.75$ at (a) $t = 20$ s and (b) $t = 50$ s in case 1.

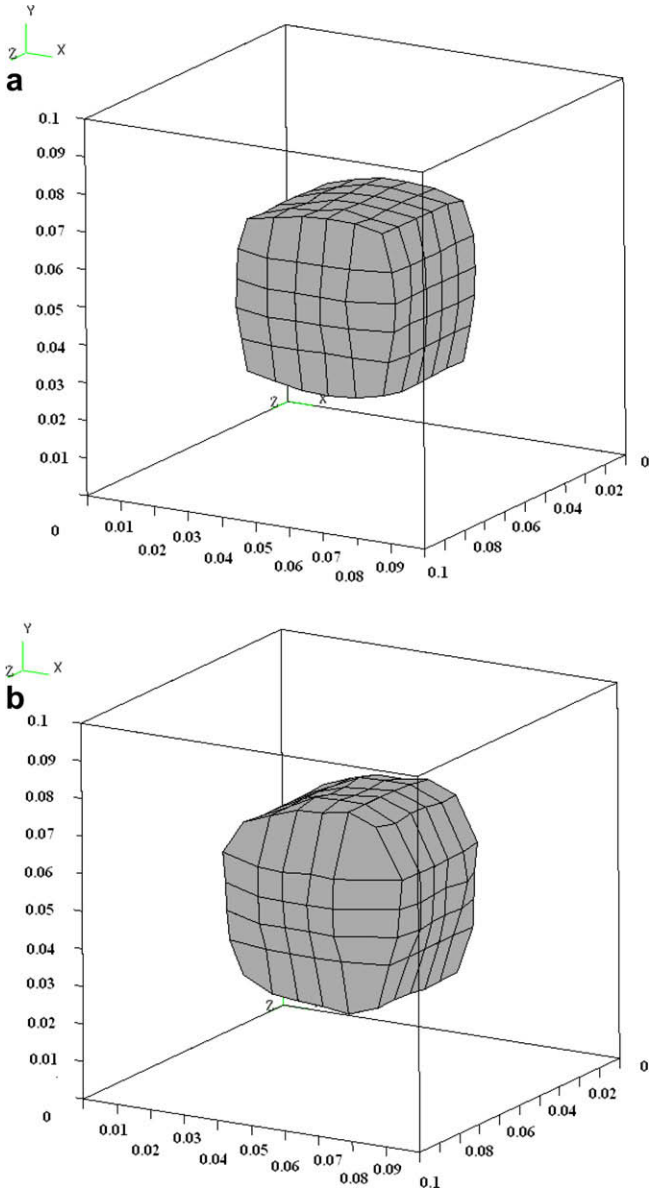

Fig. 8. The estimated cavity configurations with type A initial guess and $\sigma = 6.25$ at (a) $t = 20$ s and (b) $t = 50$ s in case 1.

can be obtained. The relative average errors ERR1 and ERR2 are calculated as ERR1 = 4.42% and ERR2 = 0.52%. Again, it can be seen from these data that this algorithm can obtain good estimation of $f(x,y,z,t)$ by choosing different initial guesses.

Finally, the influence of the measurement errors on this time-dependent shape identification problem needs be discussed. First, the measurement error for the simulated temperatures measured by imaginary infrared scanner on outer surface S_o is taken as $\sigma = 3.75$ (about 3% of the averaged measured temperature on S_o). The estimations for $f(x,y,z,t)$ can be obtained after only 14 iterations and the CPU time is about 14 h and 22 min. The relative average errors ERR1 and ERR2 are calculated as ERR1 = 1.86% and ERR2 = 0.66%, respectively. The estimated shapes of internal cavity at time $t = 20$ and 50 s are shown in Fig. 7a and b, respectively. ERR1 and ERR2 at $t = 20$ s are calculated as 0.27% and 0.77%, respectively, while at $t = 50$ s are obtained as 0.59% and 0.48%, respectively.

The measurement error for the temperatures is then increased to $\sigma = 6.25$ (about 5% of the averaged measured temperature on S_o). After only 7 iterations the estimated with CPU time 8 h and 20 min, $f(x,y,z,t)$ can be obtained and ERR1 and ERR2 are calculated as 2.79% and 1.12%, respectively. The identified shapes of internal cavity at time $t = 20$ and 50 s are illustrated in Fig. 8a and b, respectively. ERR1 and ERR2 at $t = 20$ s are calculated as 0.49% and 1.23%, respectively, while at $t = 50$ s are obtained as 1.28% and 0.77%, respectively.

From Figs. 3–8, it can be concluded that as the measurement errors are increased the accuracy of the estimated cavity shape is decreased, however, they are still reliable. Therefore the present technique provides confidence estimations for the three-dimensional time-dependent inverse geometry problems.

9.2. Numerical test case 2

In order to show the ability of this algorithm in handling more irregular shape of the internal cavity, in the second test case the exact cavity domain, $S_i = \{S_{iE}, S_{iW}, S_{iS}, S_{iN}, S_{iT}, S_{iB}\} = f(x,y,z,t)$, as shown in the following equations is considered:

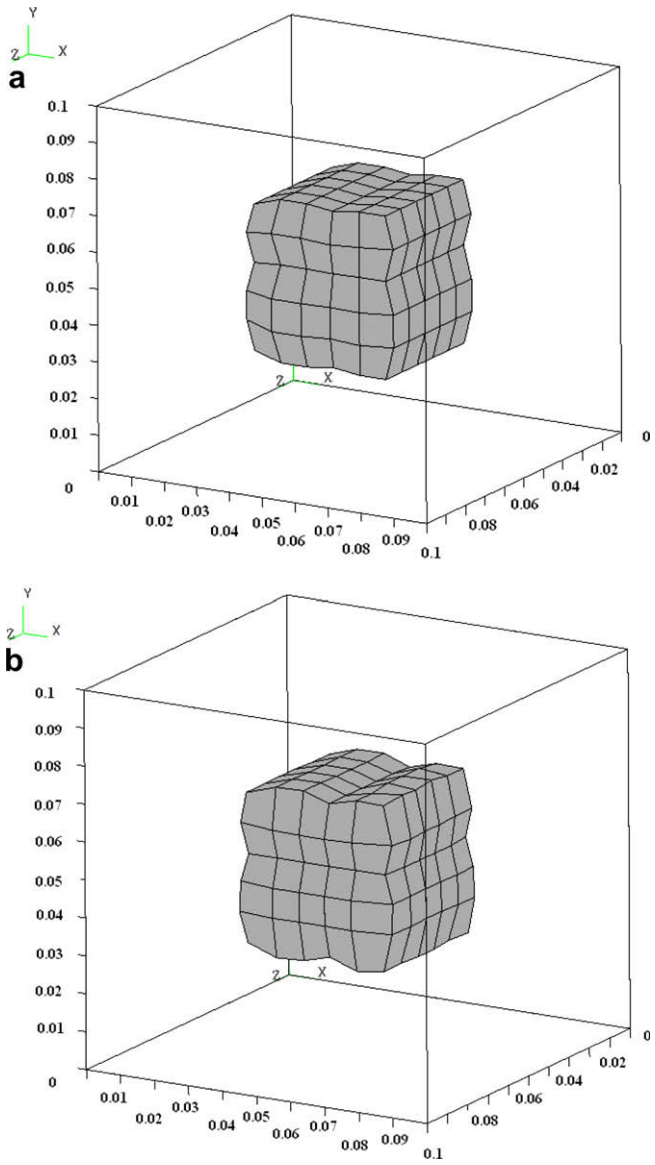

Fig. 9. The (a) exact and (b) estimated cavity configurations with type A initial guess and $\sigma = 0.0$ at time $t = 25$ s in case 2.

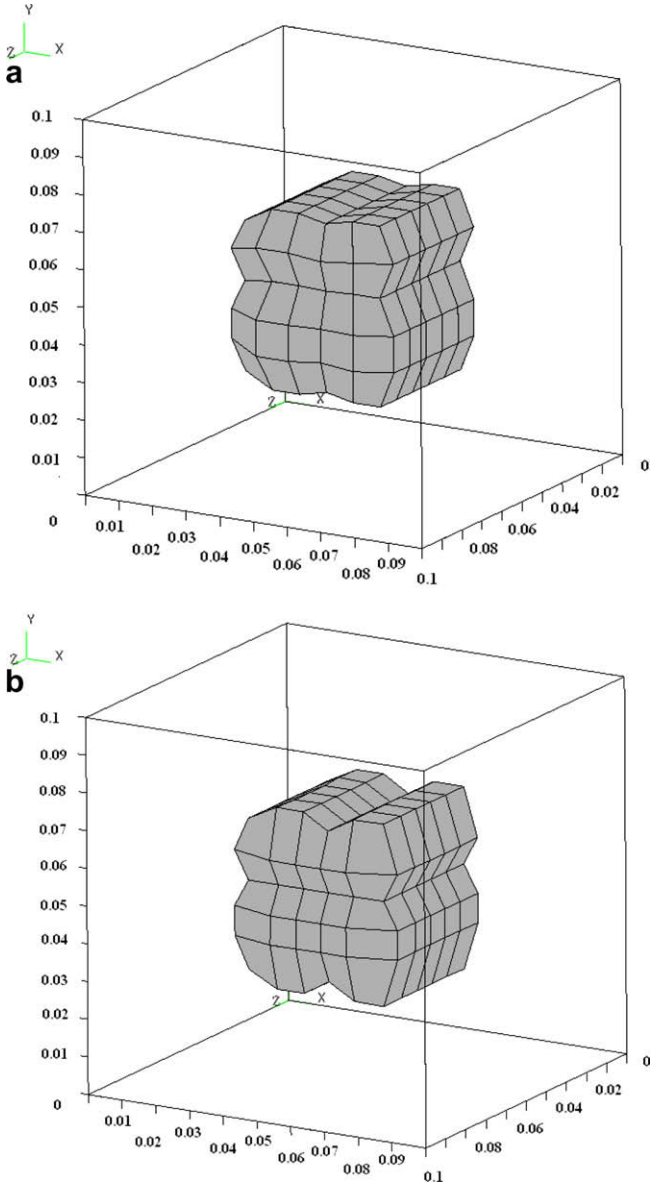

Fig. 10. The (a) exact and (b) estimated cavity configurations with type A initial guess and $\sigma = 0.0$ at time $t = 50$ s in case 2.

$$S_{iE} = 0.07 + \left\{ \left| \frac{\sin[\frac{250}{6}(y-0.03)\pi]}{110} \right| \times \sin\left(\frac{\pi t}{30}\right) \times 0.6 \right\} \quad (19a)$$

$$S_{iW} = 0.03 - \left\{ \left| \frac{\sin[\frac{250}{6}(y-0.03)\pi]}{110} \right| \times \sin\left(\frac{\pi t}{30}\right) \times 0.6 \right\} \quad (19b)$$

$$S_{iS} = 0.03 - \left\{ \left| \frac{\sin[\frac{250}{6}(x-0.03)\pi]}{110} \right| \times \sin\left(\frac{\pi t}{30}\right) \times 0.6 \right\} \quad (19c)$$

$$S_{iN} = 0.07 + \left\{ \left| \frac{\sin[\frac{250}{6}(x-0.03)]}{110} \right| \times \sin\left(\frac{\pi t}{30}\right) \times 0.6 \right\} \quad (19d)$$

$$S_{iT} = 0.07 + \left\{ \left| \frac{\sin[\frac{250}{6}(y-0.03)\pi]}{110} \right| \times \sin\left(\frac{\pi t}{30}\right) \times 0.6 \right\} \quad (19e)$$

$$S_{iB} = 0.03 - \left\{ \left| \frac{\sin[\frac{250}{6}(y-0.03)\pi]}{110} \right| \times \sin\left(\frac{\pi t}{30}\right) \times 0.6 \right\} \quad (19f)$$

First, when assuming exact measurements ($\sigma = 0.0$), using type A initial guess and choosing $\varepsilon = 7500$, after 15 iterations the estimation can be obtained and the CPU time used in inverse calculations is about 15 h and 30 min. The average relative errors for the exact and estimated cavity configurations and for the measured and estimated temperatures are calculated ERR1 = 1.31% and ERR2 = 0.18%, respectively.

The exact and estimated shapes of internal cavity by using SDM at time $t = 25$ and 50 s are shown in Figs. 9 and 10, respectively and the measured and estimated temperatures for $t = 25$ and 50 s are presented in Figs. 11 and 12, respectively. ERR1 and ERR2 at $t = 25$ s are calculated as 0.56% and 0.12%, respectively, while at $t = 50$ s are obtained as 0.57% and 0.22%, respectively. Again, the above figures and relative average errors imply that the present technique provides confidence estimation.

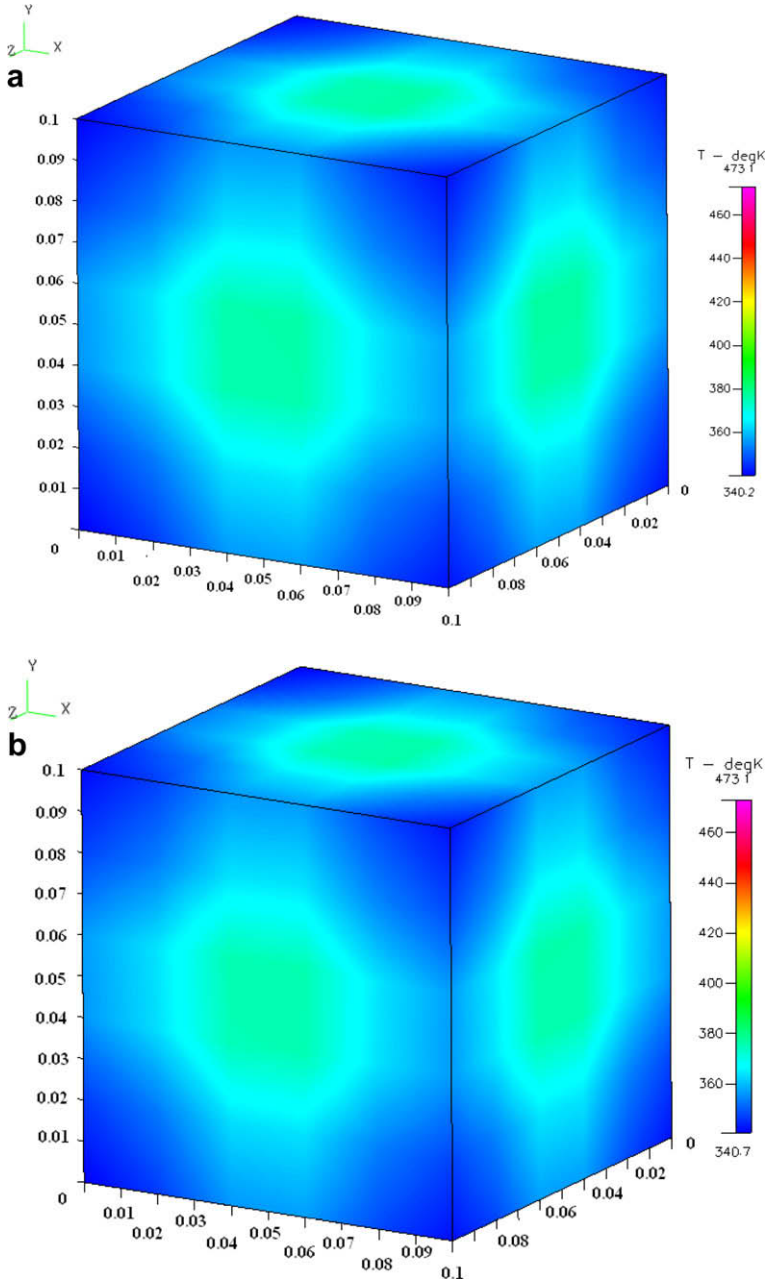

Fig. 11. The (a) simulated measured and (b) estimated surface temperatures on S_o with $\sigma = 0.0$ at time $t = 25$ s in case 2.

Next, the influence of the measurement errors need be considered and added to this time-dependent shape identification problem. First, the measurement error is taken as $\sigma = 3.6$ (about 3% of the averaged measured temperature on S_o). The estimations for $f(x,y,z,t)$ can be obtained after only 9 iterations and the CPU time is about 8 h and 51 min.

The relative average errors ERR1 and ERR2 are calculated as ERR1 = 1.59% and ERR2 = 0.65%, respectively. The estimated shapes of internal cavity at time $t = 25$ and 50 s are shown in Fig. 13a and b, respectively. ERR1 and ERR2 at $t = 25$ s are calculated as 0.51% and 0.53%, respectively, while at $t = 50$ s are obtained as 0.73% and 0.65%, respectively.

The measurement error for the temperatures is then increased to $\sigma = 6.0$ (about 5% of the averaged measured temperature on S_o). After only 5 iterations (CPU time is about 5 h and 3 min), the estimated $f(x,y,z,t)$ can be obtained and ERR1 and ERR2 are calculated as 2.09% and 1.10%, respectively. The identified shapes of internal cavity at time $t = 25$ and 50 s are illustrated in Fig. 14a and b, respectively. ERR1 and ERR2 at $t = 25$ s are calculated as 0.86% and 0.85%, respectively, while at $t = 50$ s are obtained as 1.06% and 1.12%, respectively.

From the above two numerical test cases, it can be learned that the SDM in estimating unknown space and time-dependent internal cavity does not need any assumptions for the shape of cavity such as the cubic spline fitting used in Kassab and Pollard [5]. When unknown cavity has some "sharp" corners such as in the numerical test case 2, the SDM can still be applied to obtain good estimation but a cubic spline APG algorithm may not

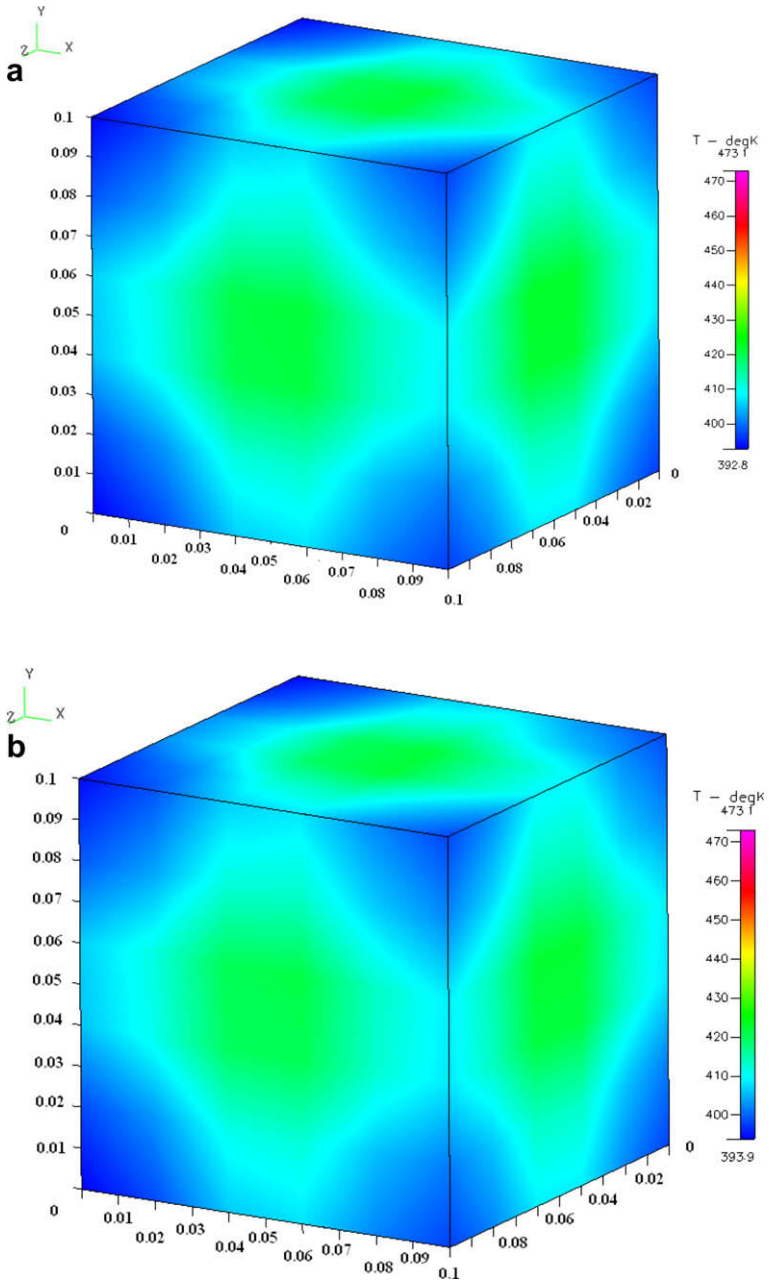

Fig. 12. The (a) simulated measured and (b) estimated surface temperatures on S_o with $\sigma = 0.0$ at time $t = 50$ s in case 2.

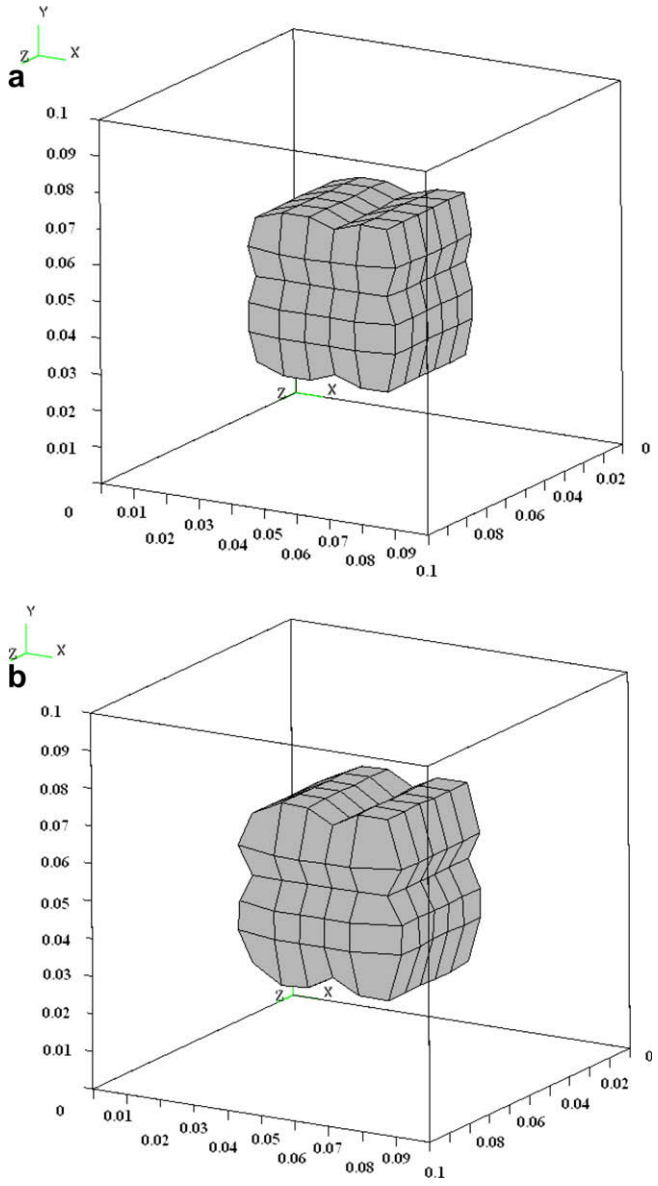

Fig. 13. The estimated cavity configurations with type A initial guess and $\sigma = 3.6$ at (a) $t = 25$ s and (b) $t = 50$ s in case 2.

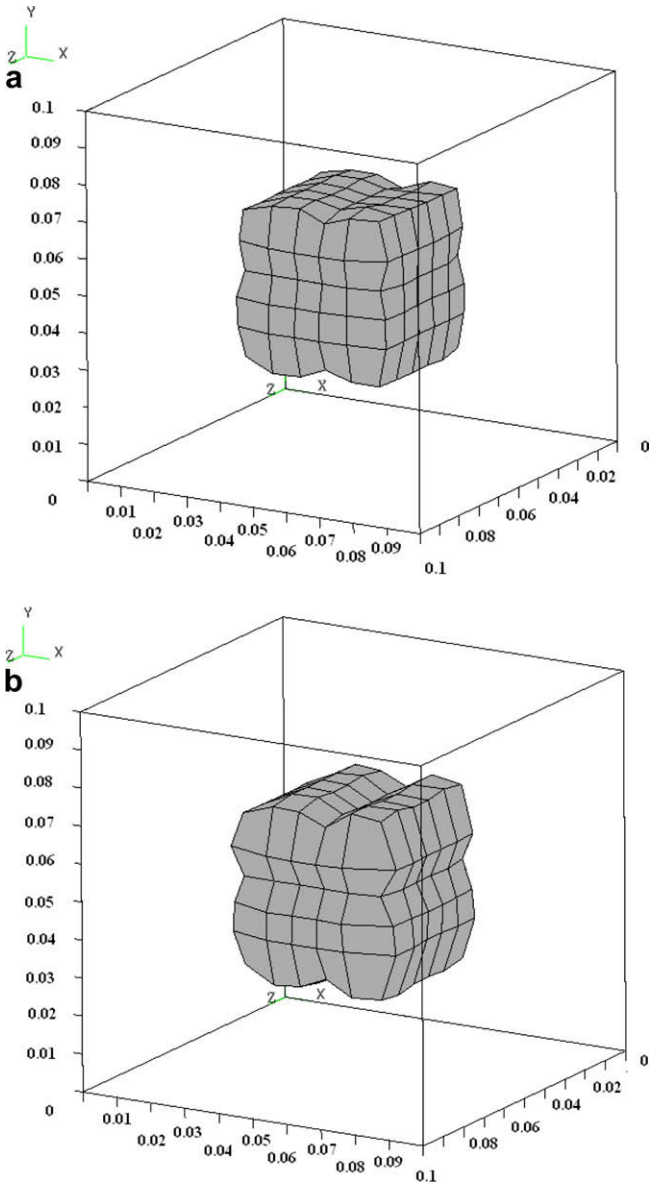

Fig. 14. The estimated cavity configurations with type A initial guess and $\sigma = 6.0$ at (a) $t = 25$ s and (b) $t = 50$ s in case 2.

perform well since cubic spline fitting cannot produce any sharp corners.

10. Conclusions

The steepest descent method (SDM) was successfully applied for the solution of the three-dimensional inverse geometry problem in estimating the unknown space and time-dependent irregular cavity configurations by utilizing surface simulated temperature measurements. Two numerical test cases involving different shape of shape of initial guess cavity, different shape of exact cavity and different measurement errors were considered. The results show that the SDM does not require an accurate initial guesses of the unknown quantities, does not need any extra assumptions such as cubic spline fitting used in Kassab and Pollard [5], needs few iterations on 586–3.0 GHz PC (on a three-dimensional problem base) and is not sensitive to the measurement errors when performing the shape estimating calculations.

Acknowledgment

This work was supported in part through the National Science Council, ROC, Grant No., NSC-96-2221-E-006-065.

References

[1] C.K. Hsieh, K.C. Su, A methodology of predicting cavity geometry based on the scanned surface temperature data-prescribed surface temperature at the cavity side, J. Heat Transfer 102 (2) (1980) 324–329.
[2] C.K. Hsieh, A.J. Kassab, A general method for the solution of inverse heat conduction problems with partially specified system geometries, Int. J. Heat Mass Transfer 29 (1986) 47–58.
[3] A.J. Kassab, C.K. Hsieh, Application and infrared scanners and inverse heat conduction methods to infrared computerized axial tomography, Rev. Sci. Inst. 58 (1987) 89–95.
[4] C.K. Hsieh, C.Y. Choi, K.M. Liu, A domain extension method for quantitative detection of cavities by infrared scanning, J. Nodes. Eval. 8 (1989) 195–211.
[5] A.J. Kassab, J. Pollard, A cubic spline anchored grid pattern algorithm for high resolution detection of subsurface cavities by the IR-CAT method, Num. Heat Transfer B 26 (1994) 63–78.
[6] K. Dems, Z. Mroz, Variational approach to sensitivity analysis in thermoelasticity, J. Thermal Stress. 10 (1987) 283–306.

[7] K. Dems, Z. Mroz, Sensitivity analysis and optimal design of external boundaries and interfaces for heat conduction systems, J. Thermal Stress. 21 (3-4) (1998) 461–488.
[8] T. Burczinski, J.H. Kane, C. Balakrishna, Shape design sensitivity analysis via material derivative-adjoint variable technique for 3D and 2D curved boundary elements, Int. J. Numer. Meth. Eng. 38 (1995) 2839–2866.
[9] T. Burczynski, W. Beluch, A. Dlugosz, W. Kus, M. Nowakowski, P. Orantek, Evolutionary computation in optimization and identification, Comput. Assist. Mech. Eng. Sci. 9 (2002) 3–20.
[10] C.H. Cheng, C.Y. Wu, An approach combining body-fitted grid generation and conjugate gradient methods for shape design in heat conduction problems, Numer. Heat Transfer B 37 (2000) 69–83.
[11] C.H. Huang, B.H. Chao, An inverse geometry problem in identifying irregular boundary configurations, Int. J. Heat Mass Transfer 40 (1997) 2045–2053.
[12] C.H. Huang, C.C. Tsai, A transient inverse two-dimensional geometry problem in estimating time-dependent irregular boundary configurations, Int. J. Heat Mass Transfer 41 (1998) 1707–1718.
[13] C.H. Huang, C.C. Chiang, H.M. Chen, Shape identification problem in estimating the geometry of multiple cavities, AIAA J. Thermophys. Heat Transfer 12 (1998) 270–277.
[14] C.H. Huang, T.Y. Hsiung, An inverse design problem of estimating optimal shape of cooling passages in turbine blades, Int. J. Heat Mass Transfer 42 (23) (1999) 4307–4319 (SCI & EI paper).
[15] C.H. Huang, H.M. Chen, An inverse geometry problem of identifying growth of boundary shapes in a multiple region domain, Numer. Heat Transfer A 35 (1999) 435–450.
[16] C.H. Huang, M.T. Chaing, A transient three-dimensional inverse geometry problem in estimating the space and time-dependent irregular boundary shapes, Int. J. Heat Mass Transfer 51 (2008) 5238–5246.
[17] E. Divo, A.J. Kassab, F. Rodriguez, An efficient singular superposition technique for cavity detection and shape optimization, Numer. Heat Transfer B 46 (2004) 1–30.
[18] CFD-ACE+ user's manual, ESI-CFD Inc., 2005.
[19] O.M. Alifanov, Inverse Heat Transfer Problems, Springer-Verlag, Berlin Heidelberg, 1994.
[20] IMSL Library Edition 10.0, User's Manual: Math Library Version 1.0, IMSL, Houston, TX, 1987.